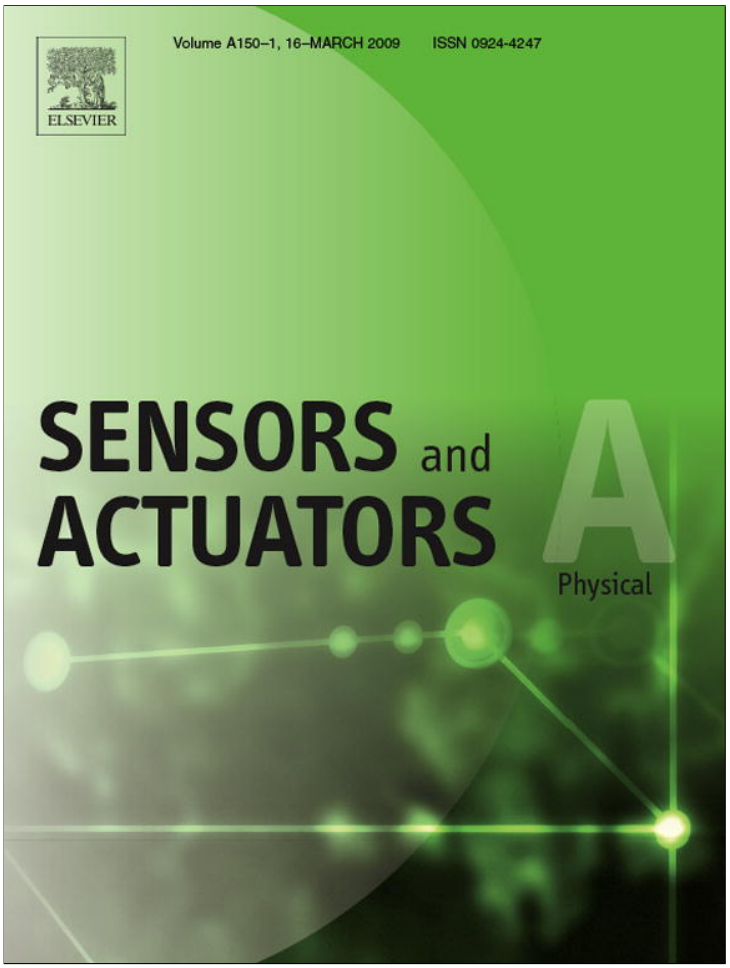

Sensors and Actuators A 150 (2009) 156–167

Contents lists available at ScienceDirect

Sensors and Actuators A: Physical

journal homepage: www.elsevier.com/locate/sna

Fabrication of gapless dual-curvature microlens as a diffuser for a LED package

C.T. Pan [a], M.F. Chen [a], P.J. Cheng [b,*], Y.M. Hwang [a], S.D. Tseng [a], J.C. Huang [c]

[a] Department of Mechanical and Electro-Mechanical Engineering, Center for Nanoscience and Nanotechnology, National Sun-Yat-Sen University, Kaohsiung 804, Taiwan, ROC
[b] Department of Electrical Engineering, Nan-Jeon Institute of Technology, Tainan County, 737, Taiwan, ROC
[c] Institute of Materials Science & Engineering, Center for Nanoscience and Nanotechnology, National Sun Yat-Sen University, Kaohsiung 804, Taiwan, ROC

ARTICLE INFO

Article history:
Received 13 March 2008
Received in revised form 2 December 2008
Accepted 14 December 2008
Available online 24 December 2008

Keywords:
Dual-curvature microlens
LED
Hot-embossing
UV-cured
Light uniformity
BMG

ABSTRACT

The light-emitting diode (LED) has been the subject of much interest in the role of a backlight module for liquid crystal displays (LCDs). However, a traditional LED lamp is a point-light source, and so is not suitable for use in large LCD panels. This study presents a new packaging method for LEDs, which uses a gapless dual-curvature microlens array (GDMLA) to improve its ability to illuminate a panel. GDMLAs of different dimensions were simulated and fabricated in order to examine their light luminance and uniformity. Commercial optical simulation software, "Tracepro", was used to obtain a GDMLA of optimized geometry and dimensions. Based on the simulated data, a GDMLA mold was first fabricated using a LIGA-like process (Lithographie Galvanoformung Abformung, LIGA); this was known as the first mold. In this study, the first mold was obtained using a nickel cobalt (Ni–Co) electroplating process. In order to obtain a highly accurate and strong mold, a bulk metallic glass (BMG) alloy, $Mg_{58}Cu_{31}Y_{11}$, was chosen as the material for the second mold, which exhibits excellent forming ability and high hardness. The pattern of the first mold was replicated onto BMG by hot-embossing, and the shrinkage between the first and the second mold was less than 0.2%. Next, the pattern of the GDMLA on the second mold was replicated onto ultraviolet (UV)-curable resin, producing the final optical film for a LED package. The shrinkage between the second mold and the UV-cured optical film was less than 0.4%; this means that the process exhibits a high replication ability. The fabricated GDMLA had the characteristics of dual curvatures and a high fill-factor of 100%. The light uniformity of the LED package with the GDMLA optical film was measured, and the results demonstrated that the GDMLA is a good optical device for use in LED packages. In addition, the relationship between the simulation and experimental results is assessed and discussed.

1. Introduction

Microlens arrays (MLAs) have been applied more and more in optical and lighting systems in recent years, such as in optical fibers, image systems and illumination. As liquid crystal displays (LCDs) have been developed quickly in a panel size, the uniformity and brightness of backlight modules have become very important. Scattering and uniformity in brightness of a light source are important issues in the field of flat panel displays, and MLAs show potential for improving scattering and the brightness of optical and lighting systems.

Many varied fabrication methods for MLAs have been described, such as the reflow process [1–3], laser-aided [4,5], gray-scale mask [6], a photothermal technique [7], molding [8,9], etching [10], surface properties [11,12], liquid crystal type [13], closed-packed colloidal monolayer [14,15], and proton beam writing [16]. A soft roller with a microlens array cavity has been made by casting a pre-polymer of polydimethylsiloxane (PDMS) in a plastic master of MLA [8]. Among these processes, molding has been identified as the process by which high replication capability, rapid fabrication and mass-production ability can be achieved with high precision. Other research on MLAs has included aspheric microlens [5], ball-lens [17] and cylindrical MLAs [18].

The fabrication of a vertical reflow microlens (VRM) has been demonstrated by the thermal reflow method; this was applied to a micro-optical/optoelectronic bench and wavelength filter [19]. A fully integrated micro-optical system was realized by laterally moving a collimating diffractive lens in the light path [20]. High-resolution imaging and beam steering using MLAs has been demonstrated [21]. Electrowetting on dielectric (EWOD) was found

* Corresponding author. Tel.: +886 6 6523112x533/32.
E-mail address: pjcheng@mail.njtc.edu.tw (P.J. Cheng).

0924-4247/$ – see front matter.
doi:10.1016/j.sna.2008.12.010

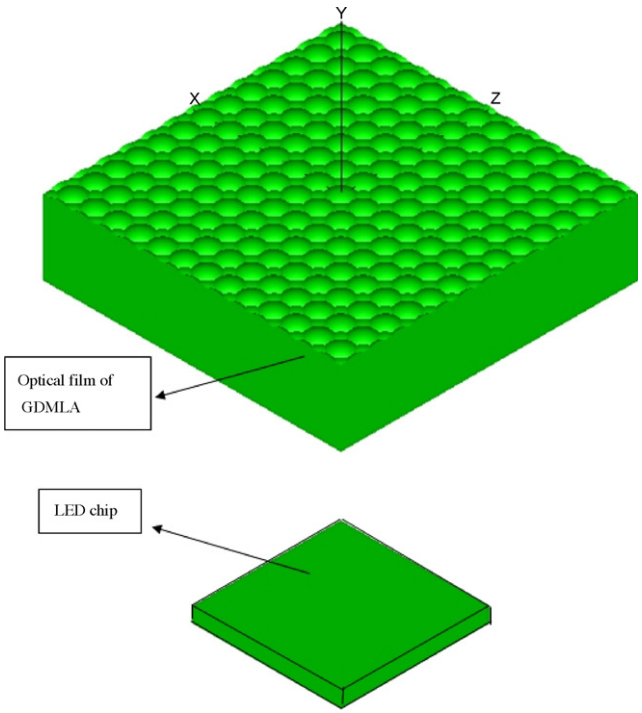

Fig. 1. Model of a LED packaged with a GDMLA optical film.

to be a promising technology for variable focal liquid microlenses, and some methods of altering the contact angle and radius have been developed: the contact angle of the liquid has been tuned with different applied voltages [22], and the radius of curvature of the microlens has tuned by liquid polymer surface tension and applied pressure [23]. Liquid droplet deposition was achieved by putting cantilevers in contact with the substrate surface [24].

An optical film with a gapless triangular microlens array (GTMLA) has also been fabricated. The PMMA-based GTMLA optical film offered a 100% fill-factor and high optical coupling efficiency to improve luminance [25,26]. PDMS microlens arrays and diffusers have been manufactured by replication molding, which can effectively expand a high-intensity laser beam [27]. A diffuser with a MLA for a light-emitting diode (LED) backlight system has been developed and was shown to enhance the color-mixing characteristics of the LED backlight system [28].

A diffuser with a high fill-factor MLA has been developed; however, there are still some optical properties in which improvement is needed. This study presents an optical film with a dual-curvature MLA as a diffuser for a LED package. The development of a mold for the replication process plays an important role in the process, and formability and hardness of the mold are critical features to consider. Thus, a bulk metallic glass (BMG), $Mg_{58}Cu_{31}Y_{11}$, was selected for use in the process. BMG is ideal due to the fact that amorphous alloys contain no dislocations that can be responsible for yielding in crystalline materials, and can therefore be expected to be strong and hard [29–34]. The material shows a very high strength at room temperature and an excellent viscous flow property at temperatures between the glass transition temperature (T_g) and the crystallization temperature (T_x). BMG has a good forming ability (GFA) at temperatures between T_g and T_x; thus, it is a good material for embossing to fabricate a mold.

In order to enhance the fill-factor of MLAs, several studies on polygonal MLAs have been conducted [9,14,35,36]; however, the curvatures of those MLAs are of a single dimension in one array. This study presents a GDMLA with two different curvatures. Optical simulation software was used to analyze the optical characteristics, and the simulation model is shown in Fig. 1. MLAs with different geometries and dimensions were simulated in order to analyze the luminance and light uniformity, which was evaluated by the standard deviation and coefficient of variation. Therefore, a MLA of better geometry and dimensions was obtained. Then, based on the analyzed data, a MLA was fabricated by a LIGA-like process

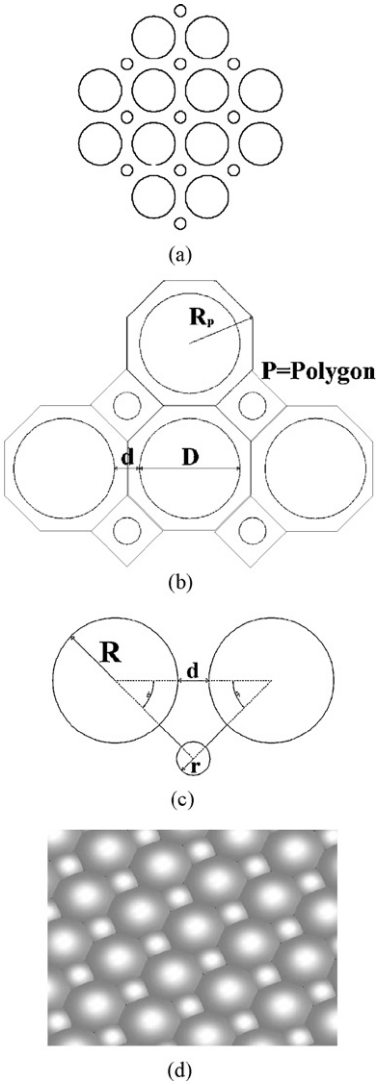

Fig. 2. Design of the photo-mask for the GDMLA: (a) layout of the photo-mask of a GDMLA; (b) the symbols of a model created to calculate the dimensions of the GDMLA; (c) the symbols of the small radius of a microlens; (d) the 3D schematic diagram of the GDMLA.

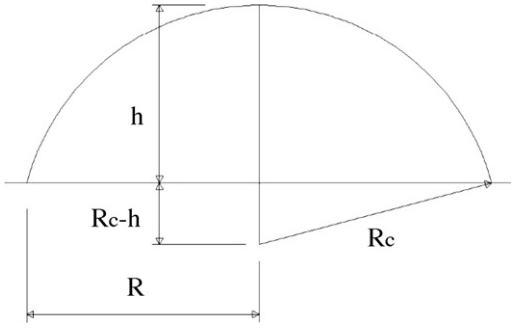

Fig. 3. Diagram of the curvature radius, photoresist thickness and microlens radius.

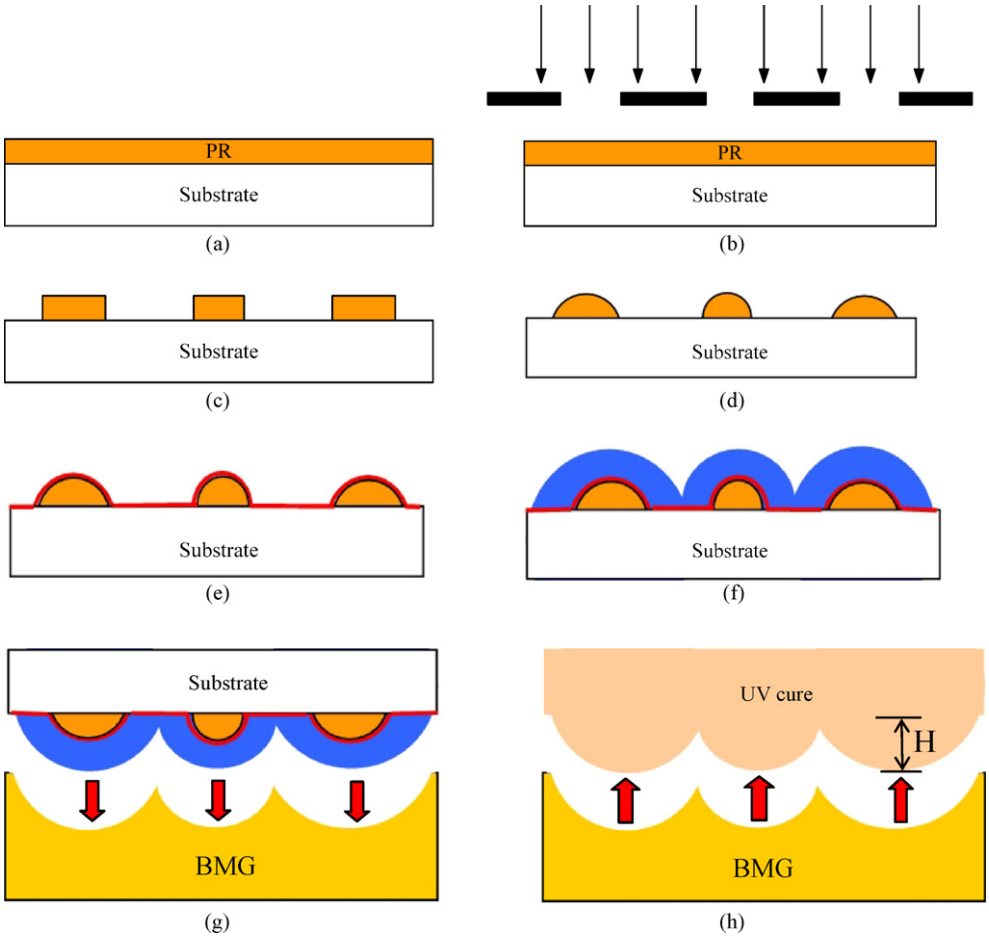

Fig. 4. Schematic flow chart of the gapless dual-curvature microlens fabrication processes: (a) AZ4620 spin-coating on the substrate; (b) lithography process; (c) the column array of different sizes on the silicon substrate after developing; (d) the column array changed to a semi-spherical array after heating the substrate at a temperature above T_g; (e) sputtered Ag as a seed layer; (f) the first mold created using a Ni–Co electroplating process; (g) the second mold of BMG created using a hot-embossing process; (h) optical film of the GDMLA using UV-curing with the BMG mold. (*H* is the thickness of the microlens as measured from the top to the film base.)

(Lithographie Galvanoformung Abformung, LIGA). The fabrication process of the gapless dual-curvature microlens array (GDMLA) included lithography, electroplating, and UV-curing. First, MLAs of different dimensions and diameters were defined using a lithography process. Then, nickel cobalt (Ni–Co) electroplating was applied to obtain an intermediate GDMLA mold, known as the first mold. Using this first mold, a second mold of BMG was replicated by a hot-embossing process, and a UV-cured process was then used to replicate the GDMLA. The second replication had a shrinkage of less than 0.4%, which means that the process is of high replication ability. The GDMLA had the properties of dual curvature and a fill-factor of 100%. Finally, the GDMLA was packaged on a LED chip to improve the luminance and uniformity. The deviation between the simulated and measured luminance and uniformity was assessed and discussed.

2. Simulation

The optical performance of different gapless polygonal MLAs, including a GDMLA, a gapless hexagonal microlens array (GHMLA)

Table 1
Detailed data obtained from three different simulation models using films of 10 μm and 20 μm thicknesses.

		Thickness (μm)					
		10			20		
		Diameter (μm)					
		60	90	120	60	90	120
GTML	Average (cd)	0.04641	0.04578	0.04572	0.04719	0.04675	0.04698
	Standard deviation	0.01748	0.01770	0.01787	0.01679	0.01679	0.01706
	C.V. (%)	37.66	38.67	39.09	35.58	35.90	36.31
GHML	Average (cd)	0.04690	0.04678	0.04657	0.04741	0.04683	0.04664
	Standard deviation	0.01655	0.01667	0.01681	0.01675	0.01637	0.01622
	C.V. (%)	35.29	35.63	36.10	35.33	34.96	34.77
GDML	Average (cd)	0.04685	0.04722	0.04712	0.04747	0.04757	0.04762
	Standard deviation	0.01645	0.01698	0.01712	0.01677	0.01693	0.01674
	C.V. (%)	35.11	35.96	36.32	35.32	35.58	35.16

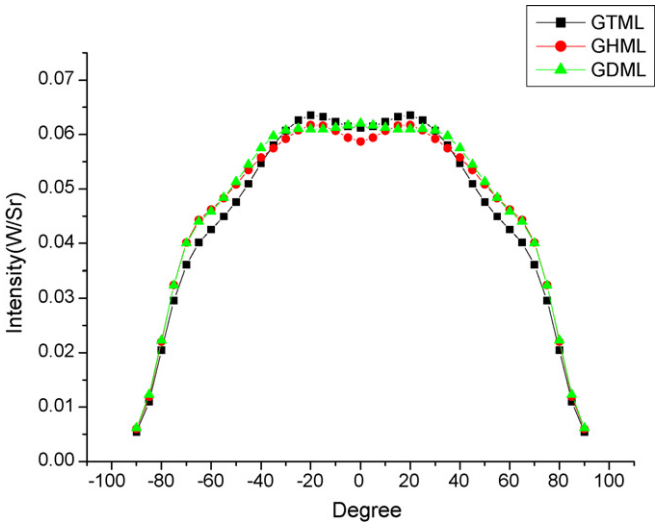

Fig. 5. Candela plots of three different arrays at a thickness of 10 μm and a diameter of 120 μm.

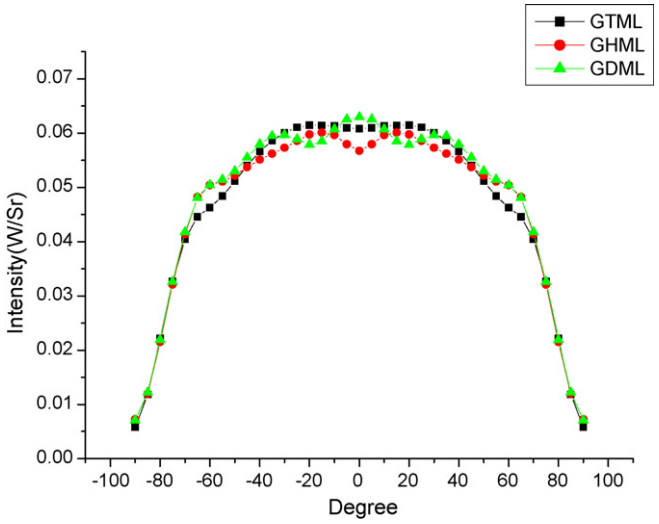

Fig. 6. Candela plots of three different arrays for a thickness of 20 μm and a diameter of 120 μm.

[9,36] and a gapless triangle microlens array [25], was compared. A simulation model of the GDMLA is shown in Fig. 1, which consisted of a LED and an optical film of a gapless polygonal MLA. The data of the luminance at different points on the LED were measured; then, based on the following Eqs. (1)–(3), which are the luminance average, standard deviation and coefficient of variation, respectively, calculations were performed in order to decide which one performed best. The larger the luminance average, the better the luminance; if the value of σ is large, the uniformity is poor; and the smaller the coefficient of variation, the better the result.

2.1. Calculation of standard variance

The arithmetic average is simplified as $\bar{X}$, whose unit is W/Sr, i.e., cd (candela), and $\bar{X}$ means the luminance average, which is the summation of all data divided by all numbers, as expressed in Eq. (1),

$$\bar{X} = \frac{\sum_{i=1}^{n} X_i}{n} \tag{1}$$

where X is a datum, n is the total number of measured data, W is Watts, and Sr is steradian. The larger the $\bar{X}$, the better the luminance.

Standard deviation (σ) is given by:

$$\sigma = \sqrt{\frac{\sum (X - X_i)}{n}} \tag{2}$$

This presents the deviation of every datum of $\bar{X}$, and so indicates the uniformity of the brightness. If σ is large, the uniformity is poor.

The coefficient of variation (C.V.) is expressed as:

$$\text{C.V.} = \frac{\sigma}{\bar{X}} \times 100\% \tag{3}$$

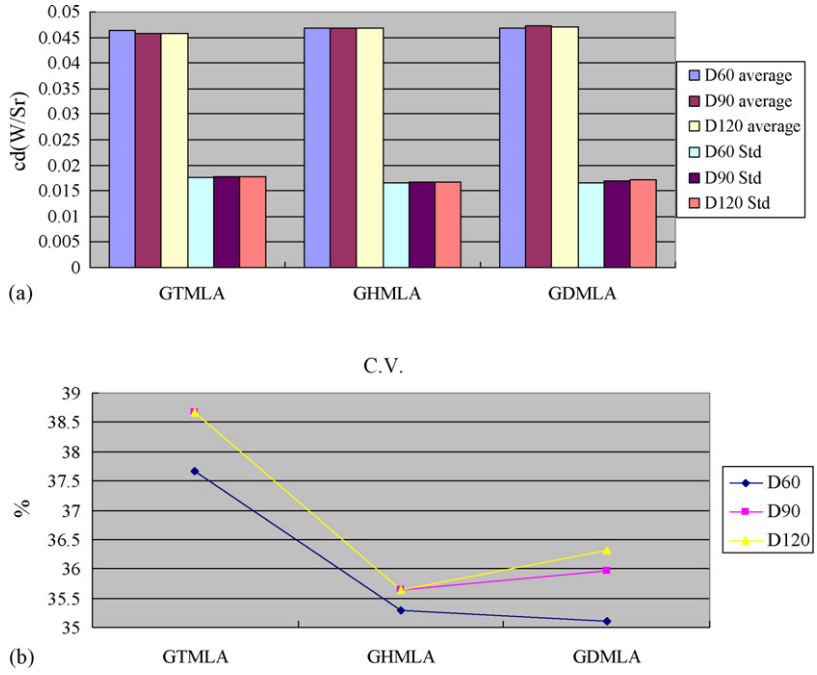

Fig. 7. Comparison of the GTMLA, GHMLA and GDMLA with three different diameters and a thickness of 10 μm: (a) the luminance average and standard deviation; (b) the coefficient of variation.

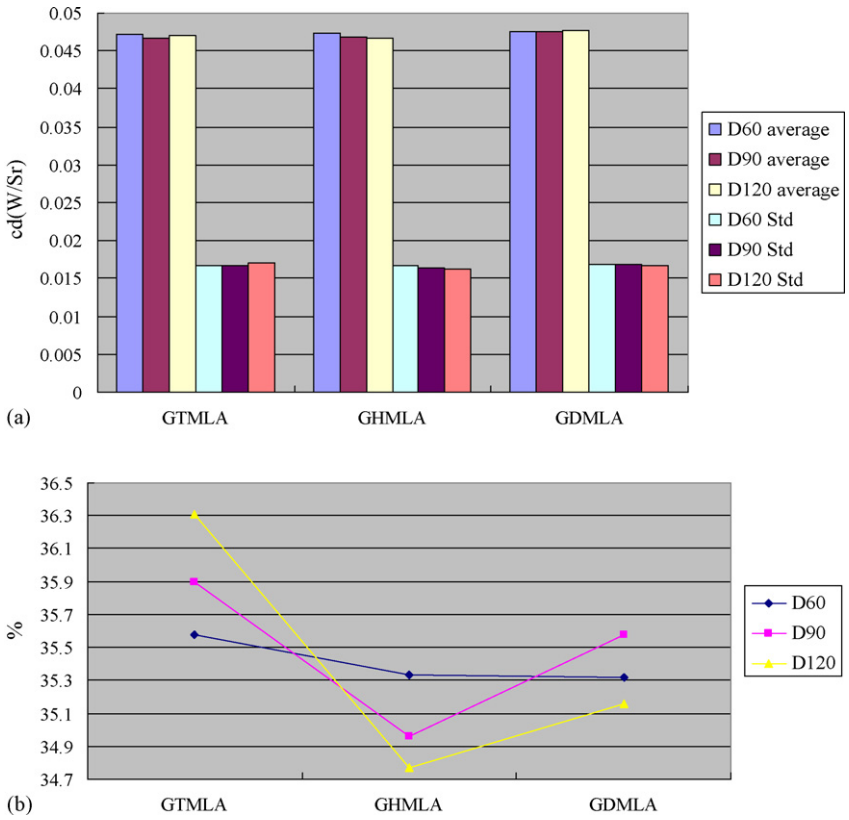

Fig. 8. Comparison of the GTMLA, GHMLA and GDMLA with three different diameters and a thickness of 20 μm: (a) the luminance average and standard deviation; (b) the coefficient of variation.

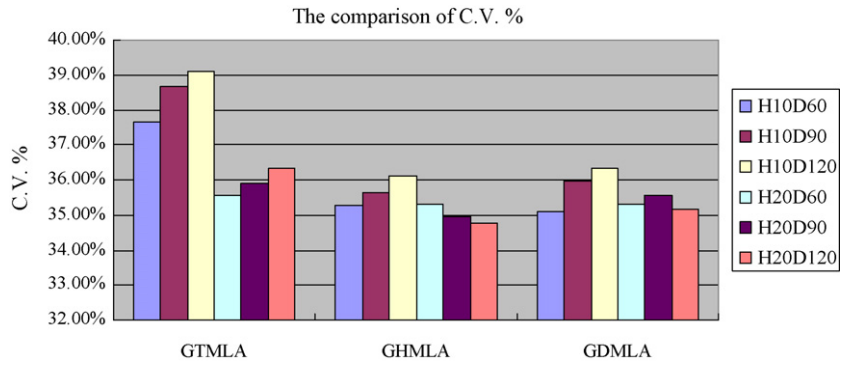

Fig. 9. Comparison of C.V. for three diameters and two thicknesses. *H* is the symbol for thickness and *D* is the symbol for diameter of the microlens.

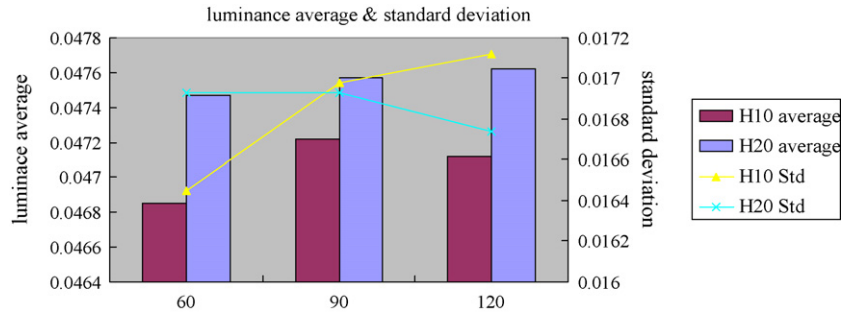

Fig. 10. GDMLA data plot showing a comparison of luminance average and standard deviation at thicknesses of 10 μm and 20 μm.

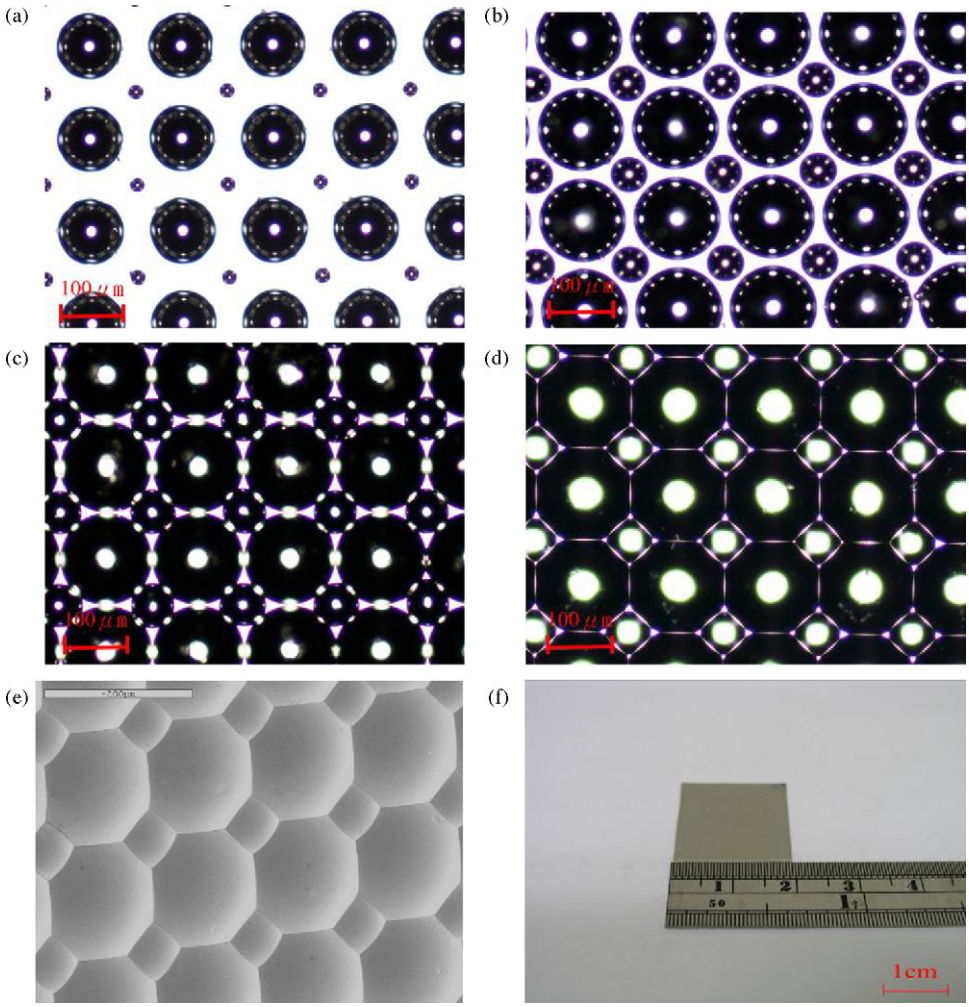

Fig. 11. (a) Sputtering of the Ag thin film as a seed layer; (b and c) the semi-spherical micolenses growing gradually due to the Ni–Co electroplating process; (d) the boundary of each microlens contacts the others to form a polygonal microlens array; (e) SEM photo of a GDMLA mold of Ni–Co alloy; (f) photo of a GDML mold of Ni–Co alloy.

This is a good index by which to indicate the variation in every factor: the smaller this index, the better the result.

2.2. Simulation model

Fig. 1 shows a simulation model created using the commercial software, Tracepro. In this model, the LED was packaged using optical film with a gapless dual-curvature microlens array. The input power of the LED was 0.45 W, and the maximum brightness was 0.9695 cd. Optical films of three different patterns, GDMLA, GHMLA and GTMLA, were tested, at thicknesses of 10 μm and 20 μm. The excircle of the polygonal microlens was 60 μm, 90 μm and 120 μm, respectively.

3. Fabrication process

A mathematical model for predicting the dimensions of the GDMLA is presented; the GDMLA was fabricated by lithography, electroplating and embossing processes.

3.1. The principles of design

The design of a photo-mask is essential in the fabrication process of GDMLAs, as it defines the final profile and dimensions of a GDMLA mold. Thus, we present a simple model for designing the dimensions of a photo-mask.

Fig. 2(a) shows the layout of the photo-mask for the GDMLA. Four circles surround a smaller one; the larger circle microlens can form an octagon after electroplating, whereas the smaller one can form a tetragon. There are two kinds of curvature within a GDMLA. A model was created to calculate the dimensions, as expressed in Eq. (4),

$$R_P = \frac{D + d}{2\cos(2\pi/2P)} \tag{4}$$

where R_p is the expected radius of the microlens, D is the diameter of the photo-mask, d is the gap between the two large circles, and P is the number of sides of the polygon (as shown in Fig. 2(b)). Then, the radius of the smaller circle (r) can be obtained from the radius of the larger circle (R) and the gap (d). The circles are crossed by a right-angled triangle (as shown in Fig. 2(c)) and a model was developed to predict r by the sine law, expressed as:

$$r = \left(2\sqrt{2} - 2\right) R + \left(\sqrt{2} - 2\right) d \tag{5}$$

Fig. 2(d) shows a 3D schematic diagram of the GDMLA, obtained using SolidWorks software. This was created based on the calculated results from Eqs. (4) and (5). The radius of curvature (R_c), thickness of photoresist (h) and the above-mentioned radius of a

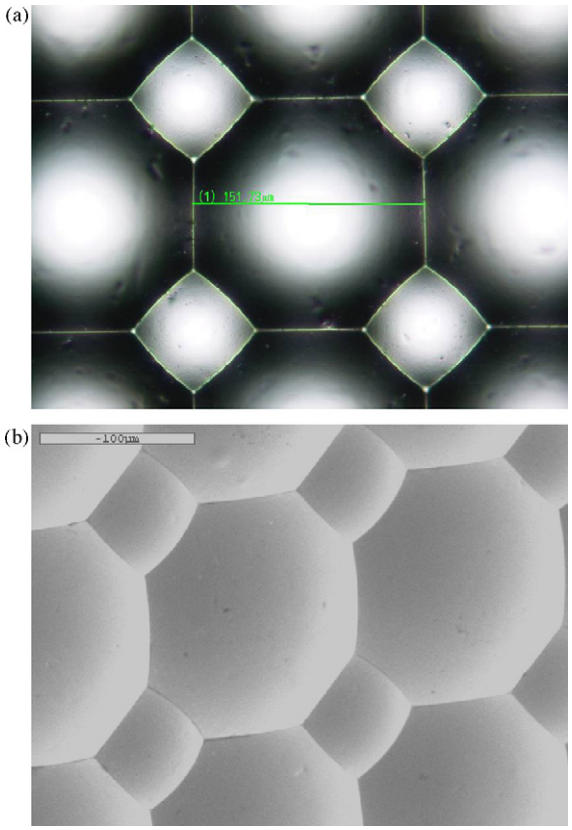

Fig. 12. Photo of a Ni–Co mold with a dimension of 151.73 μm: (a) photo by microscope; (b) photo by SEM.

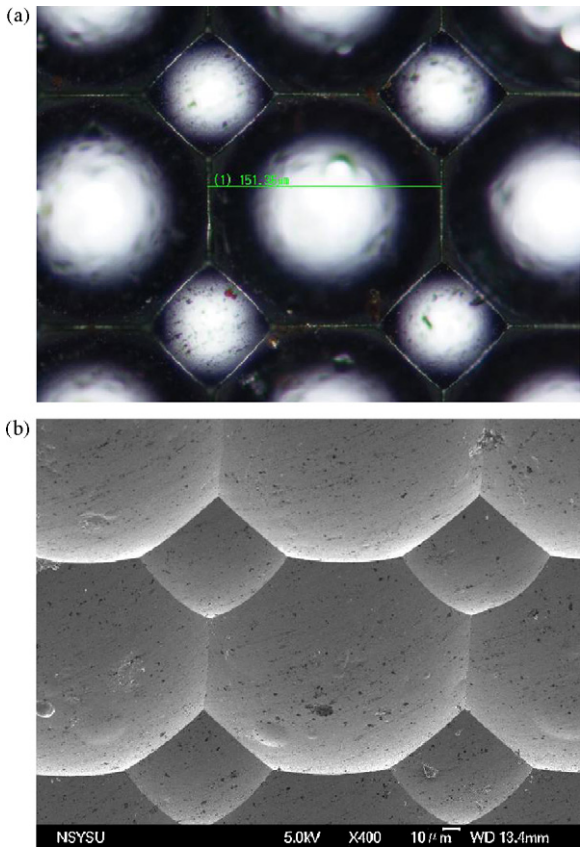

Fig. 13. Photo of a BMG mold with a dimension of 151.38 μm: (a) photo by microscope; (b) photo by SEM.

larger circle (R) are related, as shown in Fig. 3. Eq. (6) is given as:

$$R_c = \frac{h^2 + R^2}{2h} = \frac{1}{k} \tag{6}$$

where k is the curvature, the inverse of R_c.

3.2. GDMLA fabrication process

The GDMLA fabrication process was based on a LIGA-like process, and is schematically shown in Fig. 4 and described below. First, a silicon (Si) wafer was cleaned, then the photoresist was spun on the Si wafer by a spin-coating process (as shown in Fig. 4(a)), with a spinning speed of 550 rpm and duration of 15 s. After 20 min of soft baking at 90 °C, the photoresist was exposed by ultraviolet (UV) light at 360 mJ for 60 s (as shown in Fig. 4(b)). The developed patterns (see Fig. 4(c)) were placed on a hotplate and heated to 160 °C for 1 h, during which the pattern changed from a column shape to a hemi-spherical microlens (as shown in Fig. 4(d)). Then, silver (Ag) was sputtered onto the photoresist as a seed layer for the subsequent electroplating (as shown in Fig. 4(e)). Nickel cobalt (Ni–Co) electroplating was applied until the gaps between the patterns had disappeared (as shown in Fig. 4(f)). The Ni–Co alloy was of 650 Vicker Hardness (H_v), so was suitable as a first mold in the replication process. BMG has the advantageous properties of high hardness at room temperature and low viscosity at T_g; thus, the pattern on the Ni–Co mold was easily transferred to BMG, forming the second mold (as shown in Fig. 4(g)). Finally, a UV-curable polymer was spin-coated onto the BMG mold with a spinning speed of 2000 rpm and a duration of 20 s, and then cured by UV light. The GDMLA optical film was thus obtained (as shown in Fig. 4(h)).

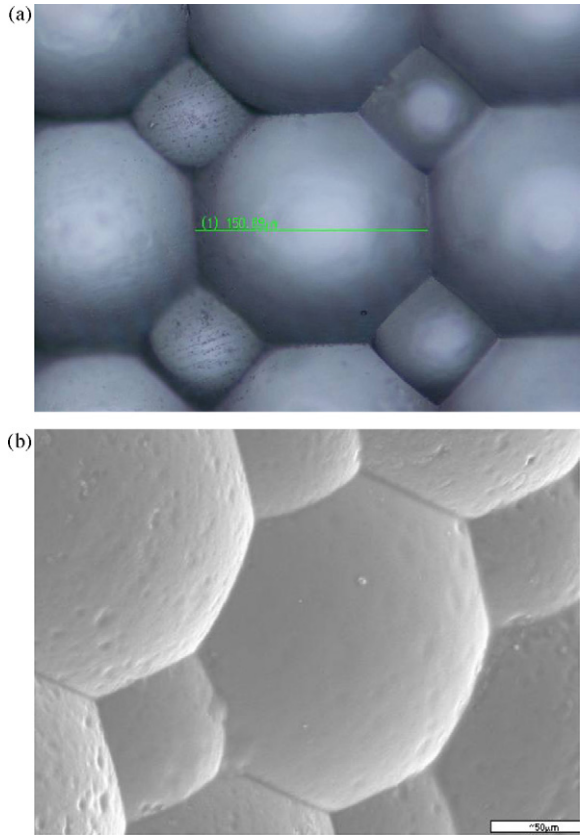

Fig. 14. Photo of a UV-cured film with a dimension of 150.69 μm: (a) photo by microscope; (b) photo by SEM.

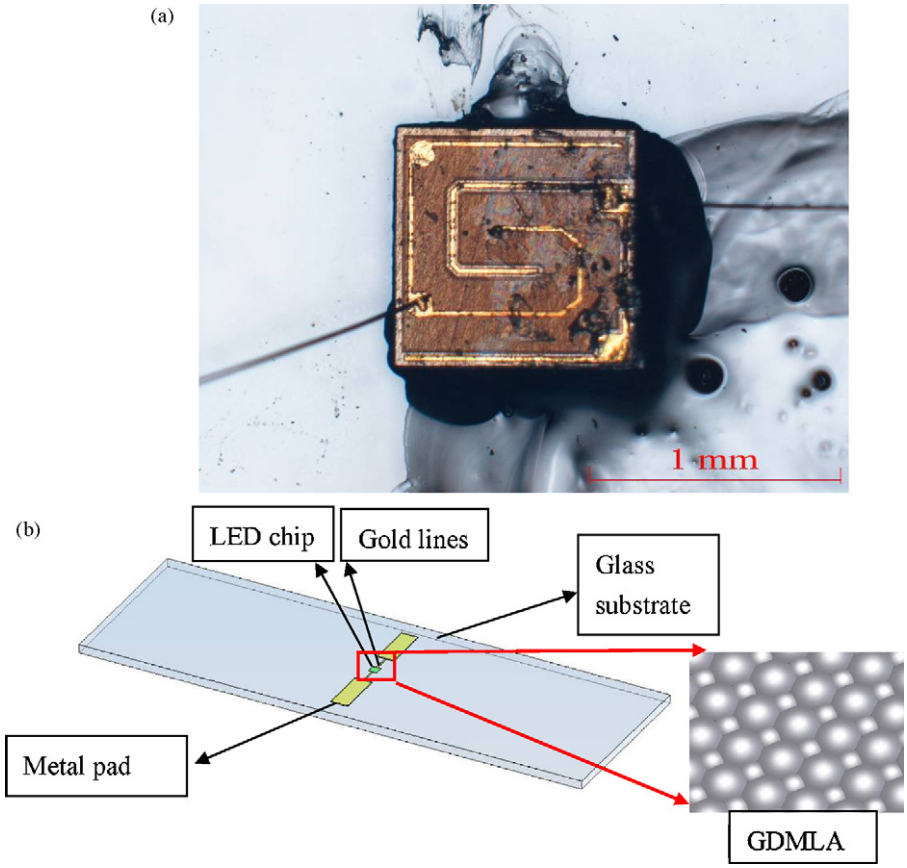

Fig. 15. (a) LED chip; (b) package of a LED chip.

4. Results and discussion

The candela plots obtained from the simulated results are shown in Figs. 5 and 6; the detailed data are listed in Table 1, which shows a comparison of three different optical films, i.e., GTMLA, GHMLA, and GDMLA, with different configurations of MLA and a thickness of 10 μm, as measured from the microlens top to the film base. The microlenses of the optical films were 60 μm, 90 μm and 120 μm in diameter, respectively. Fig. 5 shows a comparison of the three different optical films, GTMLA, GHMLA, and GDMLA, with diameters of 120 μm, which functioned as diffusers for LEDs. The distributive angle was about 140° and the brightness was quite uniform within this range. The distribution of the GHMLA and GDMLA were of a similar trend, but the GTMLA was brighter and more concentrated around the center (0°). Fig. 6 shows the same comparison between optical films of a thickness of 20 μm, as measured from the microlens top to the film base, and a diameter of 120 μm, for which the distributive angles were wider than those shown in Fig. 5.

Through calculation using Eqs. (1)–(3), the data listed in Table 1 were plotted, resulting in Figs. 7 and 8. The histograms show a comparison of the variations of the GTMLA, GHMLA and GDMLA, which revealed a similar trend. The luminance average of the GDMLA shows a maximum and the GTMLA shows a minimum. The σ of the GHMLA shows a minimum, meaning that the GHMLA has a better uniformity than the others, but the GDMLA has a greater average brightness than the others. The C.V. data of Figs. 7(b) and 8(b) were re-arranged as shown in Fig. 9, from which the difference in C.V. between the 10-μm and 20-μm films can be seen clearly. A thicker film has a better optical performance, especially the GTMLA. For 10-μm-thick films, the larger the diameter, the worse the effect; however, no regular trend was exhibited by the 20-μm-thick films. The C.V. of the GDMLA with a thickness of 10 μm and a diameter of 60 μm shows a minimum.

The GDMLA data are also plotted in Fig. 10, which reveals that the GDMLA of a thickness of 20 μm and a diameter of 120 μm exhibits a greater average brightness, and that of a thickness of 10 μm and a diameter of 60 μm has a better uniformity. The optical characteristics of the GDMLA exhibit higher averages than those of the GTMLA and GHMLA.

The fabrication process of the GDMLA was discussed previously. It involves two replication processes, i.e., from the Ni–Co mold to the BMG mold, then from the BMG mold to the final product (optical film). These processes are critical in order to obtain an accurate final product. The shrinkage rates of the materials were assessed, as given by the following equations:

$$\alpha_1 = \frac{E - H}{H} \tag{7}$$

$$\alpha_2 = \frac{H - C}{C} \tag{8}$$

where α_1 and α_2 are shrinkage rates, E is the lateral dimension of an electroplating Ni–Co mold, H is the lateral dimension of the BMG mold and C is the lateral dimension of the UV-cured final product.

Images of the evolution of the experimental electroplating process are shown in Fig. 11, from which it can be clearly seen that the circular microlens changes to a gapless polygonal microlens. After the sputtering of Ag onto the photoresist (Fig. 11(a)), Ni–Co electroplating was applied (Fig. 11(b)). The semi-spherical pattern grew slowly, then the boundaries between the pattern came into contact with each other after electroplating for 10 h (Fig. 11(c)). Finally, the gap between the semi-spherical lens disappeared and a gapless microlens array was obtained. The original circular lens changed to

a polygonal microlens due to the microlenses growing uniformly and coming into contact with each other (Fig. 11(e)). The Ni–Co mold was 2 cm × 2 cm in area (Fig. 11(f)).

An optical microscope (OM) with acquisition software and a scanning electron microscope (SEM) were used to observe the dimensions and the morphology of the mold and final product. Fig. 12(a) is a photo of the OM image of the Ni–Co mold, and shows the width to be 151.73 μm, which was averaged from at least four measurements; Fig. 12(b) is a SEM photo of the Ni–Co mold, and shows the morphology of the surface. These indicate that a GDMLA mold was successfully obtained using the electroplating process. Figs. 13(a) and 14(a) show the dimensions of the $Mg_{58}Cu_{31}Y_{11}$ BMG mold and the UV-cured optical film, respectively, which were 151.38 μm and 150.69 μm in width, respectively, averaged from at least four measurements. It was noted that the surface of the BMG mold (shown in Fig. 13(b)) was not perfect, and had some visible marks; this is because, during manufacturing of the $Mg_{58}Cu_{31}Y_{11}$ raw material using the metal casting method, some marks were produced after the quenching process, which causes roughness and oxidation on the surface. The defects of the surface of the mold can then be transferred to the final product; thus, the UV-cured optical film has several cavities on its surface (Fig. 14(b)). According to Eqs. (7) and (8), the shrinkage rates of the first and second replicas were 0.2% and 0.4%, respectively.

Finally, we used a luminance meter (BM7, TOPCON, Japan) to determine the luminance of the LED chip packaged with a GDMLA optical film. The experimental data were compared with those of the simulation. For this measurement, the LED chip was wire-bonded with gold lines as an electric conduction pad (as shown in Fig. 15(a)). Fig. 15(b) illustrates the LED configuration, and a schematic illustration of the measurement of the packaged LED is shown in Fig. 16(a). The lighting area of the LED was divided into nine portions for luminance (cd/m^2) measurement. Fig. 16(b and c) illustrates the measured data of a UV-curable optical film without

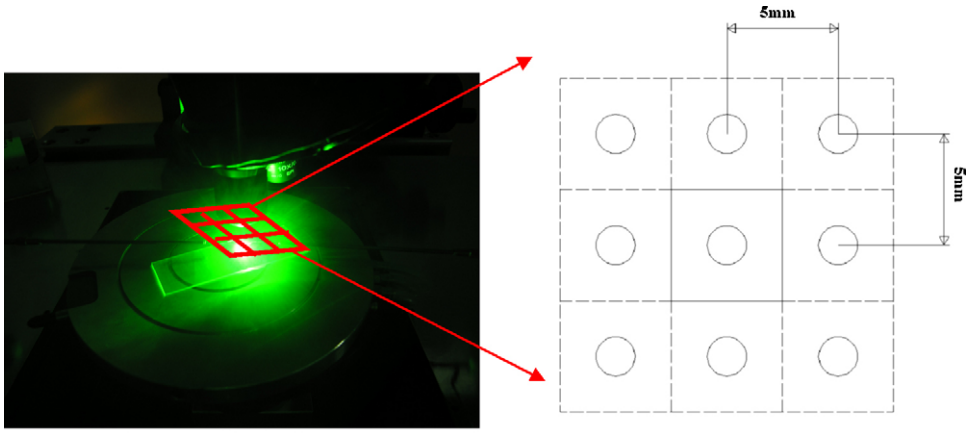

(a)

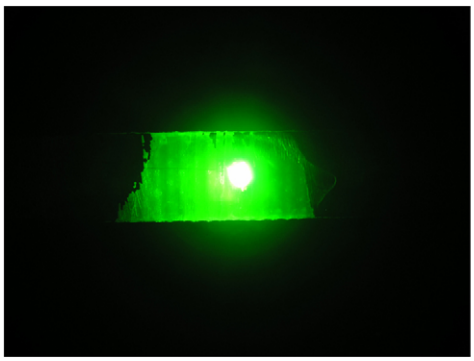

Luminance		Unit: cd/m^2
1.734×10^2	1.774×10^2	1.709×10^2
1.747×10^2	5.747×10^5	1.809×10^2
1.779×10^2	1.789×10^2	1.826×10^2

(b)

Fig. 16. The measurement setup of a LED packaged with optical film: (a) the measured point of an optical film packaged for a LED; (b) the measured data of a LED with a UV optical curable film without a GDMLA pattern; (c) the measured data of a LED with a UV optical curable film with a GDMLA pattern.

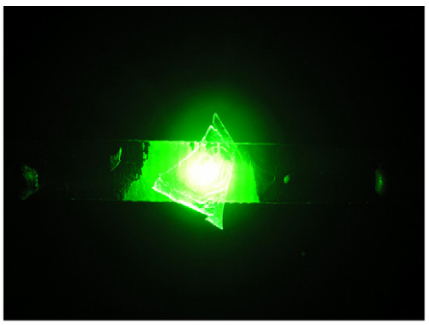

Luminance		Unit : cd/m^2
4.315×10^3	4.690×10^3	4.610×10^3
4.443×10^3 (simulated data: 1.4032×10^5)	6.461×10^5 (simulated data: 6.5442×10^5)	4.806×10^3 (simulated data: 1.5175×10^5)
4.499×10^3	4.626×10^3	4.860×10^3

(c)

Fig. 16. (*Continued*).

a GDMLA and with a GDMLA, respectively, and shows the simulation result as 6.5442×10^5 cd/m^2 and the experimental result as 6.461×10^5 cd/m^2 at the central part. The error of luminance is less than 1.2%; however, larger variation is shown at the left and right parts. This may be explained by the fact that the thin film was packaged on the LED chip with some defects, such as gaps, warpage and deflection, due to the existence of the bonding wire, and thus the measured values at the edge area are of larger deviation.

5. Conclusion

This study presents a new packaging method for LEDs using a gapless dual-curvature microlens array to enhance the illumination of a panel. The GDMLA has the properties of dual curvature and a fill-factor of 100%; it was packaged on a LED chip in order to improve the luminance and uniformity. The GDMLA was fabricated by a LIGA-like process, which included lithography, electroplating, and a UV-curing process. The first mold was obtained using a nickel cobalt (Ni–Co) electroplating process. In order to obtain a highly accurate and strong mold, $Mg_{58}Cu_{31}Y_{11}$ was chosen as the material for the second mold, which exhibits an excellent forming ability and high hardness. After the simulation data were calculated from Eqs. (1)–(3), the results revealed similar trends. However, the luminance average of the GDMLA showed a maximum and that of the GTMLA showed a minimum, and the σ of the GHMLA showed a minimum. This means that the GHMLA has a better uniformity than the others, but the GDMLA has a greater average brightness than the others. In particular, the difference in C.V. between 10-μm and 20-μm films can be seen clearly. A thicker film exhibits a better optical performance. The shrinkage between the first and the second mold was less than 0.2%, and that between the second mold and the UV-cured optical film was less than 0.4%, meaning that the process has a high replication ability. The simulation result was 6.5442×10^5 cd/m^2 and the experimental result was 6.461×10^5 cd/m^2 at the central part. The error of luminance was less than 1.2%, but larger variation is shown at the left and right parts owing to mistakes in packaging.

Acknowledgements

The authors would like to thank National Science Council (NSC) for their financial supports to the project (granted numbers: 95-2221-E-110-093-MY2, and NSC96-2622-E-110-010-CC3). Also, the authors would like to thank the Center for Micro/Nano Technology Research, National Cheng Kung University, Tainan, Taiwan, for equipment access and technical support.

References

[1] M.C. Hutley, Optical techniques for the generation of microlens arrays, Journal of Modern Optics 37 (2) (1990) 253–265.
[2] C.H. Chien, C.T. Pan, C.C. Hsieh, C.M. Yang, K.L. Sher, A study of the geometry of microball lens arrays using the novel batch-fabrication technique, Sensors and Actuators A: Physical no. 1 (2005) 55–63.
[3] C.K. Chung, Y.Z. Hong, Fabrication and analysis of the reflowed microlens arrays using JSR THB-130N photoresist with different heat treatments, Microsystems Technology 13 (2007) 523–530.
[4] J.R. Ho, T.K. Shin, J.W. Cheng, C.K. Sung, C.F. Chen, A novel method for fabrication of self-aligned double microlens arrays, Sensors and Actuators A 135 (2007) 465–471.
[5] Y.C. Lee, C.Y. Wu, Excimer laser micromachining of aspheric microlenses with precise surface profile control and optimal focusing capability, Optics and Lasers in Engineering 45 (2007) 116–125.
[6] W. Däschner, P. Long, R. Stein, C. Wu, S.H. Lee, General aspheric refractive micro-optics fabricated by optical lithography using a high energy beam sensitive glass gray-level mask, Journal of Vacuum Science & Technology B: Microelectronics and Nanometer Structures 14 (1996) 3730.
[7] N.F. Borrelli, D.L. Morse, R.H. Bellman, Photolytic technique for producing microlenses in photosensitive glass, Applied Optics 24 (16) (1985) 2520–2525.

[8] C.Y. Chang, S.Y. Yang, M.H. Chu, Rapid fabrication of ultraviolet-cured polymer microlens arrays by soft roller stamping process, Microelectronic Engineering 84 (2) (2007) 355–361.
[9] H. Yang, C.K. Chao, M.K. Wei, C.P. Lin, High fill-factor microlens array mold insert fabrication using a thermal reflow process, Journal of Micromechanics and Microengineering 14 (8) (2004) 1197–1204.
[10] P. Zhang, G. Londe, J. Sung, E. Johnso, M. Lee, H.J. Cho, Microlens fabrication using an etched glass master, Microsystems Technology 13 (2007) 339–342.
[11] W.K. Huang, C.J. Ko, F.C. Chen, Organic selective-area patterning method for microlens array fabrication, Microelectronic Engineering 83 (2006) 1333–1335.
[12] C. Tsou, C. Lin, A new method for microlens fabrication by a heating encapsulated air process, IEEE Photon Technology Letter 18 (23) (2006) 2490.
[13] H. Ren, Y.H. Lin, S.T. Wu, Flat polymeric microlens array, Optics Communications 261 (2006) 296–299.
[14] H.J. Nam, D.Y. Jung, G.R. Yi, H. Choi, Close-packed hemispherical microlens array from two-dimensional ordered polymeric microspheres, Langmuir 22 (2006) 7358–7363.
[15] F. Li, X. Li, J. Zhang, B. Yang, Enhanced light extraction from organic light-emitting devices by using microcontact printed silica colloidal crystals, Organic Electronics 8 (5) (2007) 635–639.
[16] R.K. Dutta, J.A. van Kan, A.A. Bettiol, F. Watt, Polymer microlens replication by Nanoimprint Lithography using proton beam fabricated Ni stamp, Nuclear Instruments and Methods in Physics Research, B 260 (2007) 464–467.
[17] C.C. Yang, Y.H. Huang, T.C. Peng, M.C. Wu, C.L. Ho, C.C. Hong, I.M. Liu, Y.T. Tsai, Monte Carlo ray trace simulation for micro-ball-lens-integrated high-speed InGaAS p-i-n photodiodes, Journal of Applied Physics 101 (2007) 033107.
[18] M. Ares, S. Royo, J. Caum, Shack-Hartmann sensor based on a cylindrical microlens array, Optics Letters 32 (7) (2007) 769–771.
[19] C.C. Yang, Y.H. Huang, T.C. Peng, M.C. Wu, C.L. Ho, C.C. Hong, I.M. Liu, Y.T. Tsai, Fabrication of a vertical reflow microlens with silylation technology, Sensors and Actuators A 136 (2007) 398–402.
[20] K. Hedsten, J. Melin, J. Bengstsson, P. Modh, D. Karlen, B. Lofving, R. Nilsson, H. Rodjegard, K. Persson, P. Enoksson, F. Nikolajeff, G. Andersson, MEMS-based VCSEL beam steering using replicated polymer diffractive lens, Sensors and Actuators A 142 (2008) 336–345.
[21] A. Akatay, H. Urey, Design and optimization of microlens array based high resolution beam steering system, Optics Express 15 (8) (2007) 4523–4529.
[22] Y.J. Chang, K. Mohseni, V.M. Bright, Fabrication of tapered SU-8 structure and effect of sidewall angle for a variable focus microlens using EWOD, Sensors and Actuators A 136 (2007) 546–553.
[23] Y.H. Linl, W. Hsu, A novel fabrication method of microlens array by surface tension and injection process, in: 2nd IEEE International Conference on Nano/Micro Engineered and Molecular Systems, Bangkok, Thailand, 2007.
[24] V. Bardinal, E. Daran, T. Leïchlé, C. Vergnenègre, C. Levallois, T. Camps, V. Conedera, J.B. Doucet, F. Carcenac, H. Ottevaere, H. Thienpont, Fabrication and characterization of microlens arrays using a cantilever-based spotter, Optics Express 15 (11) (2007) 6900–6907.
[25] C.T. Pan, C.H. Su, Fabrication of gapless triangular micro-lens array, Sensors and Actuators A: Physical 134 (2) (2007) 631–640.
[26] C.T. Pan, C.H. Su, Fabrication of high fill factor optical film using two-layer photoresists, Journal of Modern Optics 55 (1) (2008) 33–42.
[27] T.K. Shih, C.F. Chen, J.R. Ho, F.T. Chuang, Fabrication of PDMS(polydimethylsiloxane) microlens and diffuser using replica molding, Microelectronic Engineering 83 (2006) 2499–2503.
[28] S.I. Chang, J.B. Yoon, H. Kim, J.J. Kim, B.K. Lee, D.H. Shin, Microlens array diffuser for a light-emitting diode backlight system, Optics Letters 31 (October (20)) (2006) 3016–3018.
[29] Y.C. Chang, T.H. Hung, H.M. Chen, J.C. Huang, T.G. Nieh, Viscous flow behavior and thermal properties of bulk amorphous $Mg_{58}Cu_{31}Y_{11}$ alloy, Intermetallics 15 (2007) 1303–1308.
[30] O.N. Senkov, J.M. Scott, D.B. Miracle, Composition range and glass forming ability of ternary Ca–Mg–Cu bulk metallic glasses, Journal of Alloys and Compounds 424 (2006) 394–399.
[31] W.Y. Liu, H.F. Zhang, Z.Q. Hua, H. Wang, Formation and mechanical properties of $Mg_{65}Cu_{25}Er_{10}$ and $Mg_{65}Cu_{15}Ag_{10}Er_{10}$ bulk amorphous alloys, Journal of Alloys and Compounds 397 (2005) 202–206.
[32] Z.P. Lu, C.T. Liu, Y. Li, Glass transition and crystallization of Mg–Ni–Nd metallic glasses studied by temperature-modulated DSC, Intermetallics 12 (2004) 869–874.
[33] G. Yuan, T. Zhang, A. Inoue, Structure and mechanical properties of Mg85Cu5Zn5Y5 amorphous alloy containing nanoscale particles, Materials Letters 58 (2004) 3012–3016.
[34] G. Yuan, A. Inoue, The effect of Ni substitution on the glass-forming ability and mechanical properties of Mg–Cu–Gd metallic glass alloys, Journal of Alloys and Compounds 387 (2005) 134–138.
[35] C.P. Lin, H. Yang, C.K. Chao, Hexagonal microlens array modeling and fabrication using a thermal reflow process, Journal of Micromechanics and Microengineering 13 (5) (2003) 775–781.
[36] M.C. Chou, C.T. Pan, S.C. Shen, M.F. Chen, K.L. Lin, S.T. Wu, A novel method to fabricate gapless hexagonal micro-lens array, Sensors and Actuators A: Physical 118 (2) (2005) 298–306.

Biographies

Dr. C.T. Pan was born in Nauto, Taiwan, Republic of China, in 1969. He received his engineering degree of master and doctor in 1993 and 1998, respectively, from Power Mechanical Engineering Department of National Tsing Hua University in Hsinchu, Taiwan. He was a researcher in the field of laser machining polymer in the TU Berlin (IWF) in Germany from 1997 to 1998 and a researcher of MEMS Division in the MIRL/ITRI, Hsinchu in Taiwan from 1998 to 2003. He joined National Sun Yat-Sen University, Kaohsiung, Taiwan, Republic of China, as an assistant professor in 2003 and as an associate professor in 2005. His current research interests focus on MEMS, NEMS, and LIGA process.

M.F. Chen was born in Tainan, Taiwan, Republic of China, in 1980. He received his engineering degree of bachelor in 2003, respectively, from Mechanical Engineering Department of National Sun Yat-sen University in kaohsiung, Taiwan. He is studying in the Mechanical Engineering Research institute of Sun Yat-Sen University, Kaohsiung, Taiwan, Republic of China. His current research interests focus on MEMS, NEMS, and LIGA process.

P.J. Cheng was born in Tainan, Taiwan, Republic of China, in 1965. He received his engineering degree of master in 1994 from Mechanical Engineering Department of National Cheng Kung University in Tainan, Taiwan. He received his engineering degree of doctor in 2000 from Power Mechanical Engineering Department of National Tsing Hua University in Hsinchu, Taiwan. He joined Department of Electrical Engineering of Nan-Jeon Institute of Technology in Tainan County, Taiwan, Republic of China, as an assistant professor in 2000. His current research interests focus on MEMS, NEMS, and LIGA process.

Dr. Y.M. Hwang was born in Chanhwa, Taiwan, Republic of China, in 1958. He received his Bachelor's (1981) and Master's (1983) degrees in power mechanical engineering from National Tsing Hua University in Hsinchu, Taiwan. He earned his Doctor's degree (1990) in industrial mechanical engineering from Tokyo University in Japan. He has been a professor, Department of Mechanical and Electro-Mechanical Engineering (MEME), National Sun Yat-Sen University (NSYSU), Kaohsiung, Taiwan, since 1996. He has ever served as the department chair (2002–2005) of MEME. His research interests have been in the area of metal forming, machine design and mechanics. He won the Best Paper Award (1992) and Outstanding Engineering Professor Award (2007) from Chinese Society of Mechanical Engineers in Taiwan. He was one of the recipients of the Excellent Research Award from NSYSU in 2004.

S.D. Tseng was born in Tainan, Taiwan, Republic of China, in 1982. He received his engineering degree of Bachelor in 2005 from Mechanical Engineering Department of National Formosa University in Yunlin, Taiwan. He studied in the Mechanical Engineering research institute of Sun Yat-Sen University, Kaohsiung, Taiwan, Republic of China. His current research interests focus on MEMS and LIGA process.

Dr. J.C. Huang was born in Kaohsiung, Taiwan, Republic of China, in 1957. He received his PhD degree in 1986, from University of California, Los Angles, USA. He was a post-doc researcher in UCLA and Los Alamos National Laboratory from 1986 to 1989. He joined National Sun Yat-Sen University as an associate professor in 1989, and advanced to full professor in 1994 and chair professor in 2006. His current research interests include the metallic glasses, nano materials and composites, and transmission electron microscopy.